Journal of Engineering and Technology for Industrial Applications

ITEGAM-JETIA

Manaus, v.10 n.49, p. 104-109. September/October., 2024.
DOI: https://doi.org/10.5935/jetia.v10i49.1257

ISSN ONLINE: 2447-0228

RESEARCH ARTICLE OPEN ACCESS

A COMPARISON BETWEEN A CONVENTIONAL AND AUGMENTED RAIL GUN LAUNCHER'S PERFORMANCE

Mohamed Hichem Lahrech[1], Ahmed Chaouki Lahrech[2] and Abdelkader Bouhlal[3]

[1,2] Faculty of Technology, Ziane Achour University of Djelfa, Algeria
[3] Electrical Engineering Department. Nuclear Research Center of Birine. Djelfa, Algeria.

[1] http://orcid.org/0009-0002-5602-387X, [2] http://orcid.org/0000-0001-9738-364X, [3] http://orcid.org/0009-0000-7000-1111

Email : [1] mh.lahrach@univ-djelfa.dz, [2] ahmed.lahrech@univ-djelfa.dz, [3] aek.bouhlal@gmail.com

ARTICLE INFO

Article History
Received: August 19th, 2024
Received: September 16th, 2024
Accepted: September 16th, 2024
Published: October 04th, 2024

Keywords:
Laplace force,
Electromagnetic Launcher,
Inductance mutual coupling,
Plasma effect,
High speed Projectile.

ABSTRACT

An electromagnetic launcher is a device that uses the interaction between the magnetic fields produced by electrical currents to accelerate a projectile. Such an accelerator constitutes an alternative to the launchers propelled by chemical reactions and offers the advantage of being able to obtain very high speeds. The aim of this paper is to compare the performances of the Conventional Rail Gun (CRG) and the Augmented Rail Gun (ARG). This last is presented in the form of a launcher (CRG) reinforced by a second pair of rails, The prototype proposed is of small gauge (60 cm in length and 15 mm in diameter). The launcher's power supply is comprised of condensers' benches, which supply current to two distinct circuits: the inner circuit connects to the projectile, while the outer circuit generates an additional magnetic field. The maximum current of the inner circuit is worth 200 kA, and that of the external circuit is equal to 300 kA. The launcher makes it possible to accelerate projectiles with one or several bridges of current; the projectile mass lies between 2.0 g and 20 g.

I. INTRODUCTION

Electromagnetic launch technology is a unique form of electric propulsion that can transform electrical energy into kinetic energy. The current pulses generate an electromotive force that propels emission components, such as aircraft, missiles, satellites, rockets, and other objects, along conductive tracks at a high speed [1]. Over the past ten years, there has been extensive research and development focused on the augmented electromagnetic railgun [2-5]. Electromagnetic rail launchers are part of the electric launcher family, the simple concept involves placing a projectile between two rails connected to an electrical energy source. The current generates a magnetic field that interacts with the projectile's current. This interaction generates a Laplace force that is responsible for the projectile's movement [6-9]. In conventional electromagnetic launchers, a substantial electrical current must flow through the rails and armature in order to generate a strong electromagnetic force capable of propelling the projectile at high speed. As a result of magnetic flux diffusion, the electrical current becomes focused on the back of the armature [10], leading to a concentration of high current and the subsequent generation of heat due to the Joule effect and friction. Subsequently, they have the ability to undergo a transformation into plasma contacts. To maintain optimal efficiency, it is crucial to prevent such a transition, as it leads to a rise in the resistance of the current bridge, thereby reducing the launcher's performance. Furthermore, it significantly erodes the rails and reduces the launcher's lifespan. One alternative method to enhance muzzle velocity is by using magnetic field augmentation. This technique increases the magnetic flux in the bore, resulting in a higher accelerating force on the armature without the need to increase the current being used. Several augmentation methods, such as series-augmented and parallel-augmented, have been thoroughly studied [2], [11] and [12]. It is therefore important to limit the current intensity of the bridges without reducing the propulsive force. This can be achieved by applying an external field to the projectile's current bridges [4].

For a projectile with a current bridge (P) in an augmented launcher (Figure 1), the magnetic coenergy of the circuit is equal to:

$$W_C = \frac{1}{2}L_R I_R^2 + \frac{1}{2}L_P I_R^2 + \frac{1}{2}L_A I_A^2 + \frac{1}{2}L_P I_A^2 + M I_R I_A \qquad (1)$$

The force acting on the current bridge is determined by the virtual work method:

$$F_P = \frac{\partial W_C}{\partial x} = \frac{1}{2}\frac{\partial L_R}{\partial x} I_R^2 + \frac{\partial M}{\partial x} I_R I_A \quad (2)$$

The inductances of the external circuit, L_2 and L_p, do not vary when the projectile moves. Their partial derivative with respect to the position of the projectile is therefore zero. Let us introduce the following notations: $L'_R = \frac{\partial L_R}{\partial x}$, $M' = \frac{\partial M}{\partial x}$. The electromagnetic force on the bridge, and therefore on the projectile, is then written as:

$$F_P = \frac{1}{2} L'_R I_R^2 + M' I_R I_A \quad (3)$$

$$F_P = \frac{1}{2}\left(L'_R + 2M' \frac{I_A}{I_R}\right) I_R^2 \quad (4)$$

We can deduce the force due to the nth current

1) In the case of parallel augmentation:

$$F_{P,n,(parallel)} = \frac{1}{2}\left(L'_R + 2M'_{RA}\frac{I_A}{I_R} + 2M'_{R3}\frac{I_3}{I_R} + \ldots + 2M'_{Rn}\frac{I_n}{I_R}\right) I_R^2 \quad (5)$$

$$F_{P,n(parallel)} = \frac{1}{2}\left(L'_R + 2M'_{RA}\frac{I_A}{I_R} + \sum_{i=3}^{n} 2M'_{Ri}\frac{I_i}{I_R}\right) I_R^2 \quad (6)$$

2) In the case of series augmentation $I_A = I_R = I_n$ the force is written:

$$F_{P,n,(serie)} = \frac{1}{2}(L'_R + 2M'_{RA} + 2M'_{R3} + \ldots + 2M'_{Rn}) I_R^2 \quad (7)$$

$$F_{P,n,(serie)} = \frac{1}{2}(L'_R + 2M'_{RA} + \textstyle\sum_{i=3}^{n} 2M'_{Ri}) I_R^2 \quad (8)$$

3) In the case of the conventional launcher:
The mutual inductance M' is zero, the force then becomes:

$$F_P = \frac{1}{2} L'_R I_R^2 \quad (9)$$

II. BEHAVIOR ANALYSIS OF THE LAUNCHER OPERATING IN CRG AND ARG MODES

After modeling the CRG and ARG launchers and establishing the propulsion force equations (3) and (9). The following terms will be calculated analytically:

- L'_R: gradient of the self-inductance of the rails of the internal circuit, µH/m.
- M': gradient of the mutual inductance of the internal and external circuits, µH/m.

The launcher can be represented by an equivalent electrical circuit in Figure 3. Such a representation will make it possible to describe the evolution of the different currents circulating in the launcher (Figure 4).

In order to carry out the simulation work with the "Circuit Maker" software, it is necessary to determine the different electrical parameters of the equivalent circuit (Table 1). The objective of the simulation is to study the behavior of the launcher based on the dynamics of the projectile [6], [7]. The designed launcher can operate in CRG mode by powering only the inner rails and also in ARG mode by exciting the outer and inner rails simultaneously.

Table 1: Electrical parameters of the launcher operating in CRG and ARG modes.

Parameter	Value
Resistance of the inner rails and the projectile Rx1	0.05mΩ
Resistance of the outer rails Rx2	0.002 mΩ
Inductance of the inner rails Lx	0.5 µH
Inductance of the outer rails Lx1	1.76 µH
Connection resistance Rc and Rc1	8 mΩ
Connection inductance Lc and Lc1	1.6 µH
Storage inductance Ls	0.2µH
Wiring resistance Ri and Ri1	0.8 mΩ
Wiring inductance Li and Li1	1.6 µH
Power source for the external circuit	Capacitor bank of 0.5mf under a voltage of 8 kV.
Energy source for the internal circuit	Capacitor bank of 0.5mf under a voltage of 7 kV.

Source: Authors, (2024).

The flowchart (Figure 2) represents the different steps of the simulation to obtain the speed shape as a function of the projectile displacement; the weight of the projectile is fixed at 20 g:

1) Fixing the geometry: the outer circuit is identical to the inner circuit; the length is fixed at 60 cm.
2) Calculation of electrical parameters: the parameters are presented in the following table after the analytical calculation [7]. The parameters M' and L'_R of equation (10) are also calculated analytically: $M' = 0{,}156\mu H/m$, $L'_R = 0{,}5\mu H/m$
3) Composition of the equivalent electrical circuits of the launcher: the electrical circuit of the outer rails is identical to the inner circuit; the only values that change are the resistances and inductances of the outer rails. The augmented rail launcher is presented as two electrically independent circuits but magnetically coupled by the mutual M' via the inner and outer rails. The launcher is represented by two equivalent circuits formed by resistances and inductances. In other words, the equivalent circuit corresponding to the inner rails is only that of the launcher operating in CRG mode. The circuit of the augmented rail launcher is shown in Figure 3.
4) Evolution of the currents in the inner and outer rails of the launcher. The equivalent diagram of the launcher will then allow us to represent the evolution of the currents in the inner and outer rails (Figure 4). After determining these currents, we calculate the thrust force of the projectile (Figure 5) it should be noted that a thrust force of the order of 40 kN is obtained for a current of 300 kA flowing in the inner circuit and 330 kA in the outer circuit.

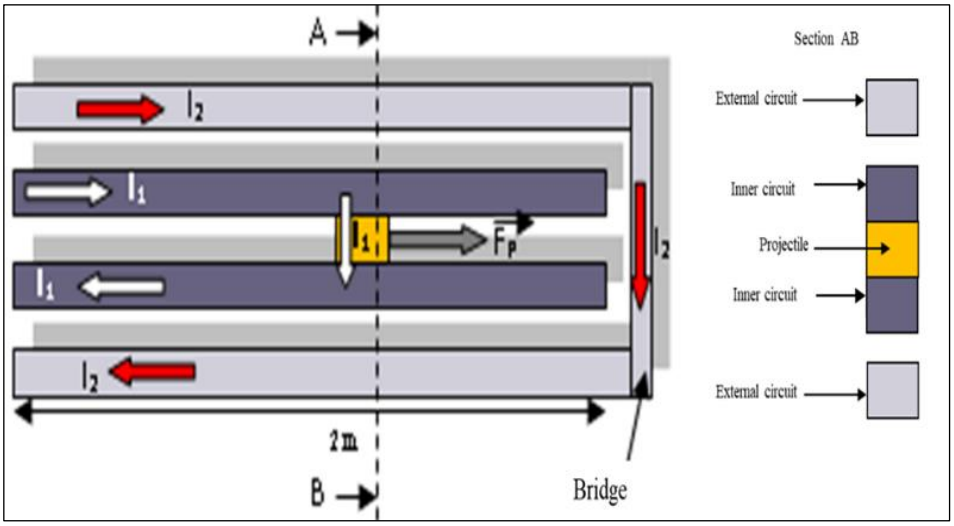

Figure 1: The projectile with a current bridge in the augmented launcher.
Source: Authors, (2024).

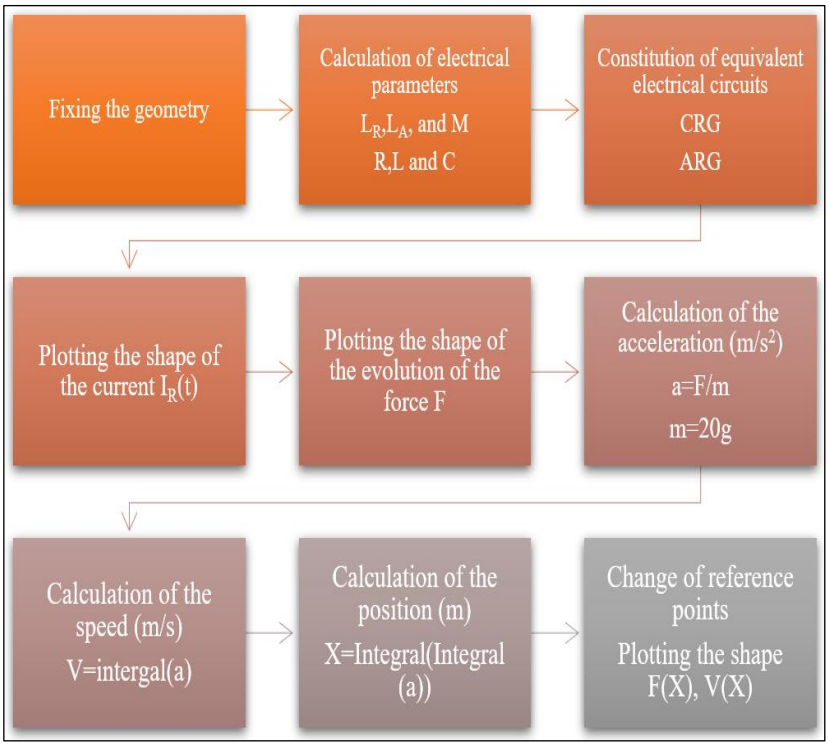

Figure 2: Simulation flowchart.
Source: Authors, (2024).

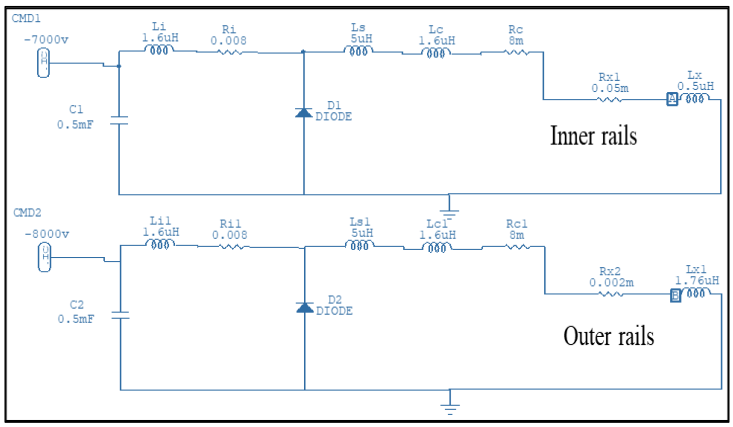

Figure 3: The equivalent electrical circuit of the launcher operating in ARG and CRG modes.
Source: Authors, (2024).

III. DYNAMICS OF THE LAUNCHER PROJECTILE OPERATING IN CRG AND ARG MODES

The determination of the instantaneous currents I_1(t) and I_2(t) in Figure 4 would allow us to calculate and represent the acceleration, speed, and evolution of the force over time.

1) Acceleration of the projectile as a function of time:
With a projectile of mass equal to 20 g, the acceleration reaches a value of 2.0×(10^6) m/s^2. (Figure 6)
2) Projectile velocity as a function of time:
The evolution of the velocity is deduced from the acceleration, and we note values of the order of 1.01 km/s. (Figure 7)
3) The ELM force and speed as a function of displacement:
In the Figure 8, we have also plotted the evolution of the force of the launcher operating in CRG mode in order to be able to make a comparison.

It is clear from the curves in Figures 8 and 9 that the maximum propulsion force is greater in the case of the launcher operating in ARG mode has a greater maximum propulsion force. The contribution of the outer rails is therefore notable through the electromagnetic mutual M between the two pairs of rails. The R_F ratio between the forces is of the order of 1.6:

$$R_F = \frac{F_{ARG}}{F_{CRG}} \tag{10}$$

The comparison of the performances of the two types of launchers shows that a clear improvement of more than 60% is observed. The architecture of the launcher with two pairs of rails proves to be a very practical solution for the propulsion of projectiles at high speeds. This architecture is more convincing with a better choice of the ratio between the currents circulating in the inner and outer rails.

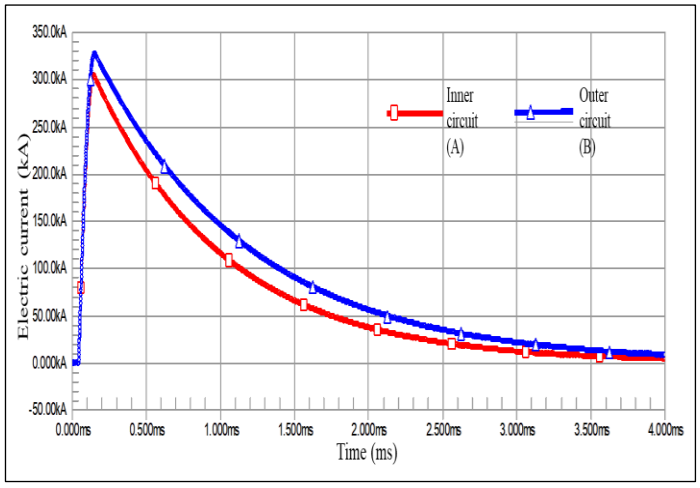

Figure 4: The simulated currents at points (A) and (B), (A: inner rails) and (B: outer rails).
Source: Authors, (2024).

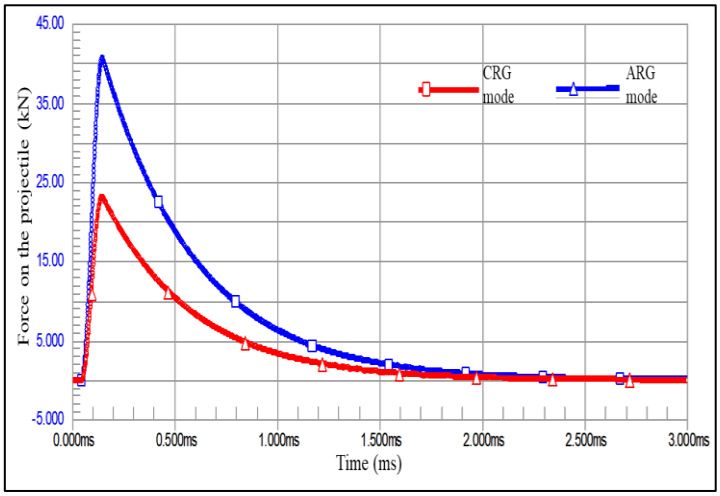

Figure 5: Comparison between forces on the projectile (kN) as a function of time (ms). (CRG and ARG modes).
Source: Authors, (2024).

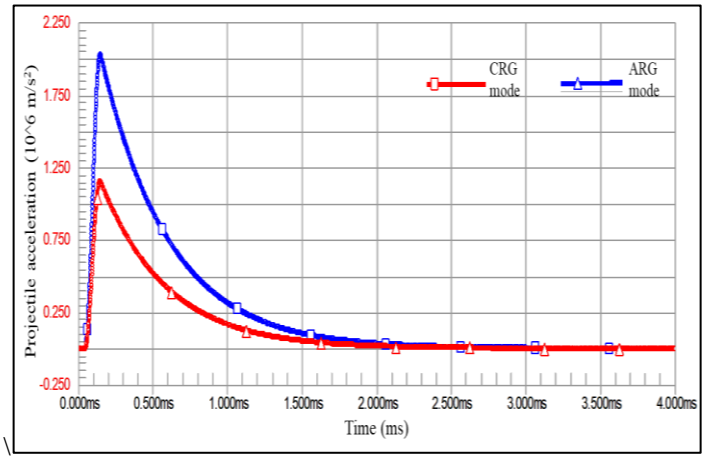

Figure 6: Comparison between projectile accelerations (10^6 m/s^2) as a function of time (ms). (CRG and ARG modes).
Source: Authors, (2024).

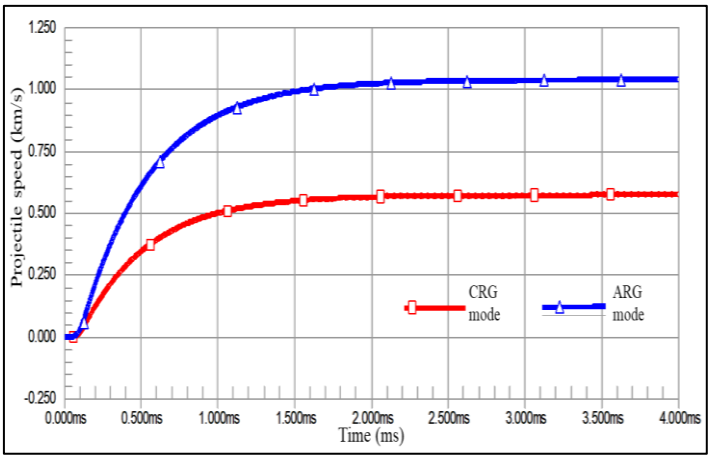

Figure 7: Comparison between the projectile speeds (km/s) as a function of time (ms) (CRG and ARG modes).
Source: Authors, (2024).

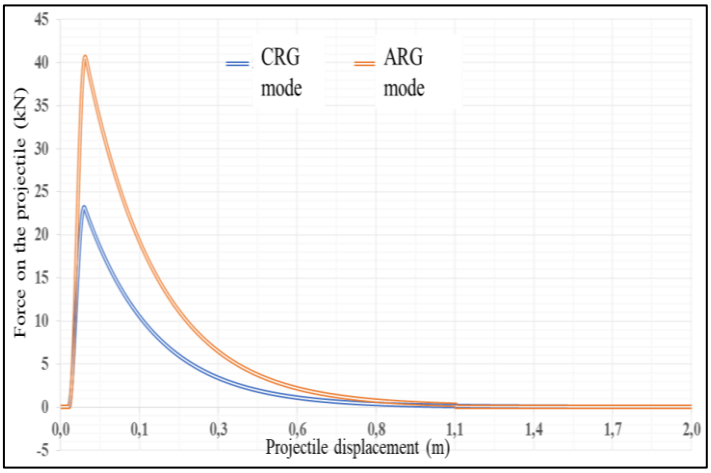

Figure 8: Comparison between the ELM forces of CRG and ARG as a function of the projectile displacement along the length of the rails in meters.
Source: Authors, (2024).

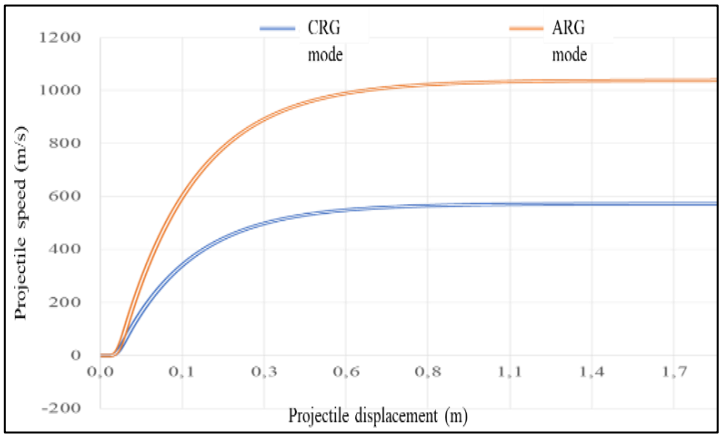

Figure 9: Comparison between the projectile speeds as a function of its displacement along the rails (CRG and ARG modes).
Source: Authors, (2024).

IV. PROTOTYPE PRODUCTION

After the analytical study carried out previously, a prototype was produced with rounded section rails. With such a shape, the propulsion force is greater compared to that obtained with rectangular section rails. Indeed, the results obtained by the researchers at the Saint Louis Institute have shown that the inductance gradient responsible for the force is better in the case where the rails have a rounded shape [6].

This launcher has two pair of rails with a rounded shape on the inside and outside (Figure 10), with dimensions represented in Table 2:

Table 2: dimensions of inner and outer rails.

	Length (cm)	Radius (cm)	Opening angle	Thickness (mm)
Inner rails	60	0.75	75°	3
Outer rails	60	1.5	75°	3

Source: Authors, (2024).

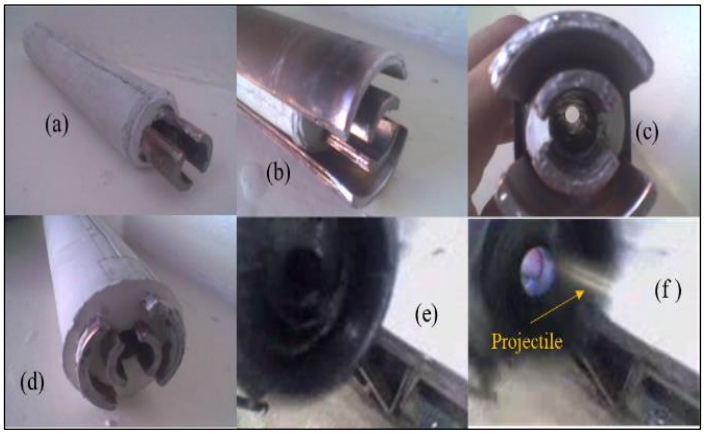

Fig 10: Augmented rail launcher prototype, (a) a pair of rounded shape copper for inner rails placed in a ceramic mold (CRG mode), (b) additional pair of rounded shape copper for outer rails superposed on inner rails (ARG mode), (c) cross-sectional view of launcher, (d) two pairs of rails placed in a ceramic mold (ARG mode), (e) the launcher Muzzle before the launch, (f) the launcher muzzle after the launch of the projectile.
Source: Authors, (2024).

In Figure 11, the four rails of the launcher must have connection terminals in the form of connecting cables, allowing different connections, of the series or parallel type. To this end, the two output ends (mouths) of the two outer rails are linked, and the ends of the two inner rails appear as free electrical terminals.

Figure 11: Augmented Rail Launcher Wiring.
Source: Authors, (2024).

The first test was unsuccessful, which was predictable because of the heating of the electrical contact parts between the projectile (Figure 12a) and the inner rails. This heating occurs mainly during the short duration (pulse) of the electrical supply (Figure 12b),[13]. We recommend techniques to address this phenomenon effectively. It is useful to mention a judicious technique for reducing the concentrations of high current densities in the multifilament contact regions. The projectile is equipped with contacts in the form of a brush[1], [6].

For our part, we have opted for a solution that consists of using a system that will propel the projectile at the same time as the electrical pulse supplying the rails. This assistance system is in the form of a breech comprising a spring and a piston in a cylindrical jacket (Figure 13). Following the pre-accelerator assembly, we recorded 12/16 successful shots; Figure 14 illustrates the projectile's exit through the launcher's muzzle.

We recorded an average speed of 507 m/s for CRG mode and 800 m/s for ARG mode with Doppler radar. We noticed a speed increase of 57%, which is very close to the theoretical value. Unfortunately, the enormous friction of the projectile on the rails and the excessive heat from the plasma prevented us from achieving speeds near the theoretical value. All of these phenomena reduce the launcher's performance. After all these results, we can deduce the efficiency of the launcher, which is equal to 80%.

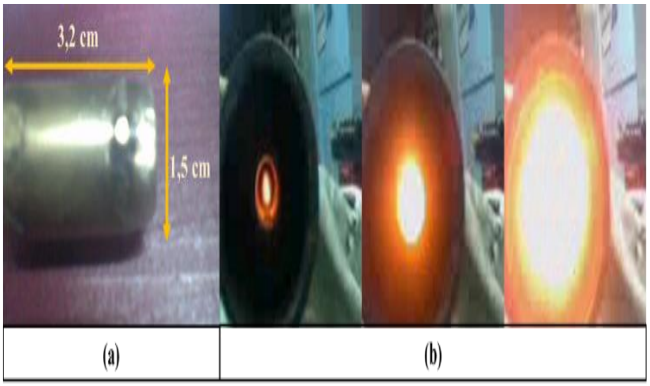

Figure 12: Projectile of the augmented rail launcher: (a) dimensions of the projectile,
(b) the heating of the electrical contact parts between the projectile and the inner rails.
Source: Authors, (2024).

Figure 13: Final assembly of the augmented rail launcher.
Source: Authors, (2024).

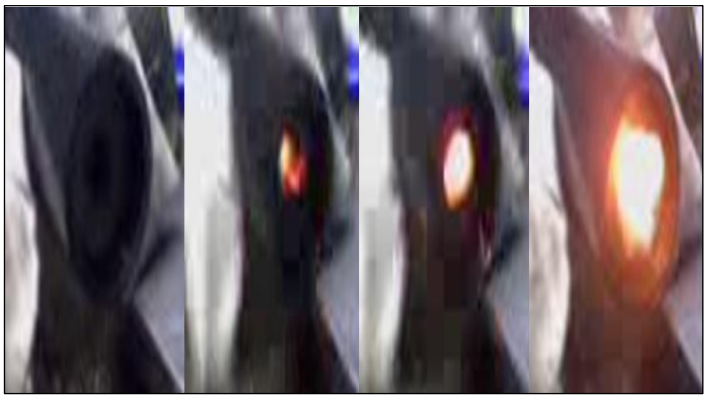

Figure 14: Firing sequences with the augmented rail launcher.
Source: Authors, (2024).

V. CONCLUSION

Despite the lack of electrical energy used, we adopted a pre-accelerator in order to avoid the problem of welding the projectile. The simulation calculation and experimental results shows that the increase in rails allows for a 60% increase in propulsion force. Certainly, the increase in rails presents itself as a solution to improve the propulsion of the projectile while also remedying the heating problems caused by high current concentrations.

We believe that through our humble work, we have contributed to the opening of the field of study of the rail launcher, where several works can be considered on the improvement of performance by the simultaneous association of solutions relating to the increase and arrangement of the rails, their power supply, and the adaptation of technologies.

VI. AUTHOR'S CONTRIBUTION

Conceptualization: Mohamed Hichem Lahrech, Ahmed Chaouki Lahrech and Abdelkader Bouhlal.
Methodology: Mohamed Hichem Lahrech and Abdelkader Bouhlal.
Investigation: Mohamed Hichem Lahrech, Ahmed Chaouki Lahrech and Abdelkader Bouhlal.
Discussion of results: Mohamed Hichem Lahrech, Ahmed Chaouki Lahrech and Abdelkader Bouhlal.
Writing – Original Draft: Mohamed Hichem Lahrech and Ahmed Chaouki Lahrech
Writing – Review and Editing: Mohamed Hichem Lahrech and Ahmed Chaouki LAHRECH
Resources: Mohamed Hichem Lahrech, Ahmed Chaouki Lahrech and Abdelkader Bouhlal.
Supervision: Mohamed Hichem Lahrech, Ahmed Chaouki Lahrech and Abdelkader Bouhlal.
Approval of the final text: Mohamed Hichem Lahrech and Ahmed Chaouki Lahrech.

VIII. REFERENCES

[1] V. Vertelis, G. Vincent, M. Schneider, S. Balevičius, V. Stankevič, et N. Žurauskiene, « Magnetic Field Expulsion From a Conducting Projectile in a Pulsed Serial Augmented Railgun », *IEEE Transactions on Plasma Science*, vol. 48, nº 3, p. 727-732, mars 2020,doi: 10.1109/TPS.2020.2970764.

[2] T. G. Engel, « The High-Efficiency Mode of Electromagnetic Launcher Operation », *IEEE Transactions on Plasma Science*, vol. 48, nº 4, p. 1106-1110, avr. 2020, doi: 10.1109/TPS.2020.2978202.

[3] Q. Lin et B. Li, « Field-Circuit Coupled Analysis of a Series-Augmented Electromagnetic Railgun », *IEEE Transactions on Plasma Science*, vol. 48, nº 6, p. 2287-2293, juin 2020, doi: 10.1109/TPS.2020.2991160.
[4] C. Li *et al.*, « Simulations on Saddle Armature With Concave Arc Surface in Small Caliber Railgun », *IEEE Transactions on Plasma Science*, vol. 47, nº 5, p. 2347-2353, mai 2019, doi: 10.1109/TPS.2019.2894165.

[5] M. B. Heydari, M. Asgari, et A. Keshtkar, « A Novel Structure of Augmented Railgun Using Multilayer Magnets and Sabots », *IEEE Transactions on Plasma Science*, vol. 47, nº 7, p. 3320-3326, juill. 2019, doi: 10.1109/TPS.2019.2921222.

[6] J. Gallant et P. Lehmann, « Experiments with brush projectiles in a parallel augmented railgun », *IEEE Transactions on Magnetics*, vol. 41, nº 1, p. 188-193, janv. 2005, doi: 10.1109/TMAG.2004.838988.

[7] M. Coffo et J. Gallant, « Modelling of a Parallel Augmented Railgun with Pspice Validation of the Model and Optimization of the Augmenting Circuit », in *2007 IEEE 34th International Conference on Plasma Science (ICOPS)*, juin 2007, p. 1020-1020. doi: 10.1109/PPPS.2007.4346326.

[8] P. Lehmann, H. Peter, F. Jamet, et V. Wegner, « Some remarks concerning the optimization of a railgun system », *IEEE Transactions on Magnetics*, vol. 31, nº 1, p. 546-551, janv. 1995, doi: 10.1109/20.364635.

[9] P. D. Aalto et F. Y. Yee, « Plated armature contacts for solid armature electromagnetic railgun launchers », *IEEE Transactions on Magnetics*, vol. 31, nº 1, p. 667-672, janv. 1995, doi: 10.1109/20.364614.

[10] X. Fu, D. Zhang, W. Yuan, et P. Yan, « Design and Analysis of the 270-kJ PPS for Augmented Railgun », *IEEE Transactions on Plasma Science*, vol. 45, nº 7, p. 1496-1502, juill. 2017, doi: 10.1109/TPS.2017.2705839.

[11] T. G. Engel, J. M. Neri, et M. J. Veracka, « Characterization of the Velocity Skin Effect in the Surface Layer of a Railgun Sliding Contact », *IEEE Transactions on Magnetics*, vol. 44, nº 7, p. 1837-1844, juill. 2008, doi: 10.1109/TMAG.2008.922310.

[12] H. Kashii, M. Yamada, et T. Shikura, « Pre-accelerator design by estimation of erosion », *IEEE Transactions on Magnetics*, vol. 27, nº 1, p. 56-60, janv. 1991, doi: 10.1109/20.100993.

[13] J. Gallant, T. Vancaeyzeele, B. Lauwens, B. Wild, F. Alouahabi, et M. Schneider, « Design Considerations for an Electromagnetic Railgun Firing Intelligent Bursts to Be Used Against Antiship Missiles », *IEEE Transactions on Plasma Science*, vol. 43, nº 5, p. 1179-1184, mai 2015, doi: 10.1109/TPS.2015.2416774.